



Contents lists available at ScienceDirect

Earth and Planetary Science Letters

www.elsevier.com/locate/epsl



Lithospheric expression of geological units in central and eastern North America from full waveform tomography

Huaiyu Yuan^{a,*}, Scott French^a, Paul Cupillard^{a,1}, Barbara Romanowicz^{a,b,c}

^a Berkeley Seismological Laboratory, Berkeley, CA 94720, United States

^b Collège de France, Paris, France

^c Institut de Physique du Globe, Paris, France

ARTICLE INFO

Article history:

Accepted 30 November 2013

Available online xxxx

Editor: P. Shearer

Keywords:

seismic tomography

lithosphere

upper mantle

surface waves

craton

eastern North America

ABSTRACT

The EarthScope TA deployment has provided dense array coverage throughout the continental US and with it, the opportunity for high resolution 3D seismic velocity imaging of both lithosphere and asthenosphere in the continent. Building upon our previous long-period waveform tomographic modeling in North America, we present a higher resolution 3D isotropic and radially anisotropic shear wave velocity model of the North American lithospheric mantle, constructed tomographically using the spectral element method for wavefield computations and waveform data down to 40 s period. The new model exhibits pronounced spatial correlation between lateral variations in seismic velocity and anisotropy and major tectonic units as defined from surface geology. In the center of the continent, the North American craton exhibits uniformly thick lithosphere down to 200–250 km, while major tectonic sutures of Proterozoic age visible in the surface geology extend down to 100–150 km as relatively narrow zones of distinct radial anisotropy, with $V_{sv} > V_{sh}$. Notably, the upper mantle low velocity zone is present everywhere under the craton between 200 and 300 km depth. East of the continental rift margin, the lithosphere is broken up into a series of large, somewhat thinner (150 km) high velocity blocks, which extend laterally 200–300 km offshore into the Atlantic Ocean. Between the craton and these deep-rooted blocks, we find a prominent narrow band of low velocities that roughly follows the southern and eastern Laurentia rift margin and extends into New England. We suggest that the lithosphere along this band of low velocities may be thinned due to the combined effects of repeated rifting processes and northward extension of the hotspot related Bermuda low-velocity channel across the New England region. We propose that the deep rooted high velocity blocks east of the Laurentia margin represent the Proterozoic Gondwanian terranes of pan-African affinity, which were captured during the Rodinia formation but left behind after the opening of the Atlantic Ocean. Our results suggest that recurring episodes of tectonic events that are well exposed at the surface also leave persistent scars in the continental lithosphere mantle, marked by isotropic and radially anisotropic velocity anomalies that reach as deep as 100–150 km.

© 2013 Elsevier B.V. All rights reserved.

1. Introduction

Our knowledge of the upper mantle shear velocity structure beneath eastern and central North America (NA) has been limited due to the lack of dense seismic station coverage. This part of the NA continent has been subjected to less recent deformation than the southern and western borders, although it has been marked by several important episodes of tectonic events in the early history of the continent construction (Fig. 1(a)): the 1.92–1.77 Ga Trans-Hudson Orogeny, which represents plate collision between

the Archean Wyoming, Hearn and Superior provinces, and is often compared to the present day Himalayas; the 1.71–1.68 Ga Yavapai and 1.70–1.65 Mazatzal orogenies, which correspond to the accretional addition of juvenile volcanic arcs to the cratonic core (Hoffman, 1988), and to the east, the 1.1 Ga Grenville and 260 Ma Appalachian orogenies, which correspond to the formation and breakup of supercontinents Rodinia and Pangea, respectively (Thomas, 2006).

In recent continental scale tomographic models, a thick cratonic root of fast shear velocity is imaged down to 200–250 km under the craton (e.g., Marone et al., 2007; Nettles and Dziewoński, 2008; Bedle and van der Lee, 2009; Yuan et al., 2011). While localized studies generally confirm this (e.g., Darbyshire and Lebedev, 2009; Chu et al., 2012; Frederiksen et al., 2013), rapid lateral changes in the velocity structure and thinning of the lithosphere have been observed towards the eastern continental margin (e.g., van der

* Corresponding author. Present address: Macquarie University, Australia. Tel.: +61 08 64369453.

E-mail address: huaiyu.yuan@mq.edu.au (H. Yuan).

¹ Present address: University of Lorraine, Laboratoire GeoRessources, ENSG, 2 rue du Doyen Marcel Roubault, 54500 Vandoeuvre-les-Nancy, France.

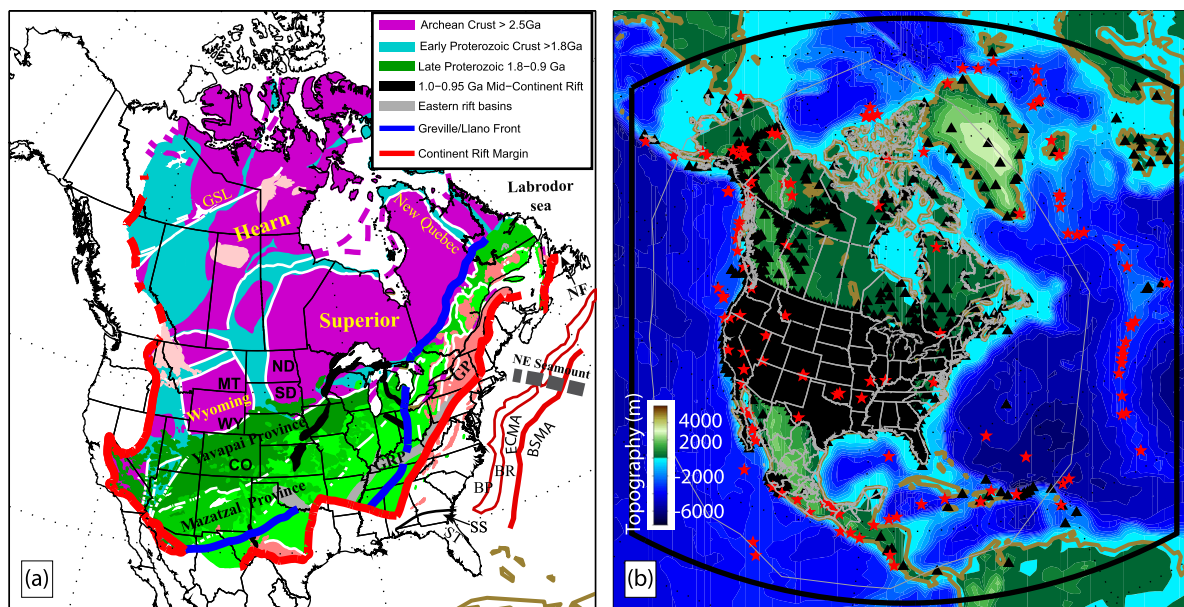


Fig. 1. (a) North American crustal provinces simplified from Whitmeyer and Karlstrom (2007). Archean and paleo-Proterozoic blocks are shaded in purple and blue in the north, while the series of southern Proterozoic provinces are shaded in green and pink. Thick red lines separate the continental core from exotic accretionary terranes. The thick blue line follows the Grenville/Llano deformation front. White lines show sutures/thrust faults. Labels are: BK, Blake Plateau; BR, Blake Ridge; BSMA, Blake Spur Magnetic Anomaly; ECMA, East Coast Magnetic Anomaly; GP, Grenville Province; GRP, Granite/Rhyolite Province; GSL, Great Slave Lake suture; NE Seamount, New England Seamount; NF, New Foundland; SS, Suwannee Suture; and ST, Suwannee Terrane. State abbreviations are: CO, Colorado; MT, Montana; ND, North Dakota; SD, South Dakota; and WY, Wyoming. (b) Source and station distribution for the new North American inversion. Black triangles show the seismic stations. Red stars are 136 local events which contribute to the new 40 s waveforms in addition to our 60 s global (French et al., 2013) and North American dataset (Yuan et al., 2011). Thick black line indicates the boundaries used for the RegSEM forward simulation, which extends 89° horizontally and down to 1600 km and contains all event-to-station paths in the 40 s dataset. The thin gray polygon indicates our model region in which the V_s and ξ structure is determined. Background shows the topography. (For interpretation of the references to color in this figure legend, the reader is referred to the web version of this article.)

Lee and Nolet, 1997; Levin et al., 2000; Rondenay et al., 2000; Menke and Levin, 2002; Li et al., 2003; Frederiksen et al., 2013). The uniquely dense coverage of the EarthScope Transportable Array (TA) in the central and eastern US opens up the opportunity to image upper mantle velocity structure at unprecedented resolution from coast to coast, which helps further our understanding of the tectonic history of the North American continent, i.e. the process of assembly of the craton and subsequent reworking of its borders. Here we show that the signature of distinct tectonic events preserved in the crust is also present in the lithospheric upper mantle down to depths reaching 150 km or more.

In this study, we present a new high-resolution 3D tomographic model of shear velocity and radial anisotropy in the cratonic North American mantle, developed using long-period full waveform inversion. This study builds upon our previous continental scale tomographic modeling efforts (Marone et al., 2007; Marone and Romanowicz, 2007; Yuan and Romanowicz, 2010b; Yuan et al., 2011). A salient feature of our previous models is the definition of the lithosphere–asthenosphere boundary (LAB) based on the variation with depth of azimuthal anisotropy: in the NA craton, the fast velocity axis changes direction towards the present day absolute plate motion direction below a depth of 180–240 km. Above the LAB the anisotropy is therefore “frozen-in” in the lithosphere, which moves as a whole over the presently deformed asthenosphere. This transition in anisotropy corresponds to a zone of strong negative gradient in isotropic shear velocity, which, however, occurs over a depth range that is too wide to be detected by high frequency methods sensitive to sharp discontinuities, such as P and S wave receiver functions and SS precursors. Further exploring the depth variations of the LAB, and better constraining the absolute values of shear velocities in the lithospheric layers is therefore a worthy goal as the Transportable Array progresses towards the eastern edge of the continent.

2. Tomographic inversion: data and methodology

The new inversion shares many methodological features with our previous continental scale time-domain three-component waveform tomographic inversions for isotropic and radially anisotropic structure (Marone et al., 2007; Yuan et al., 2011). Readers are referred to previous papers (Marone et al., 2007; Yuan et al., 2011) for the theoretical background of the regional waveform tomographic inversion methodology. Below, we highlight significant aspects of the new regional inversion.

Similar to previous inversions, the regional model is embedded in an existing global tomographic model, which serves to correct waveforms for 3D structure effects outside of the region studied. Here the global model considered is the most recent global radially anisotropic shear velocity model, SEMum2 (French et al., 2013), a second generation high resolution waveform-based model of the upper mantle developed using the spectral element method (SEM). In our previous regional studies, only teleseismic records were used, and the records were low-pass filtered at 60 s. Observed waveforms were partitioned into wave packets, allowing us to assign equal weights to fundamental modes and overtones. These wavepackets were then compared to synthetics computed using non-linear asymptotic coupling theory (NACT; Li and Romanowicz, 1995), a method based on normal mode perturbation theory which includes across branch mode coupling, resulting in 2D finite frequency waveform kernels in the vertical plane containing the source and the receiver.

Here, in addition to the 60 s low-pass filtered waveform data from ~360 global events observed on global seismic networks (used in French et al., 2013; referred to as “the 60 s global dataset”) and ~600 global events observed at NA stations (used in Yuan et al., 2011; referred to as “the 60 s NA dataset”), we further include waveforms from 136 North American regional events (Fig. 1(b)) which surround our study area (including TA stations

up to Jan 2013), filtered down to 40 s (referred to as “the 40 s NA dataset”), in order to improve both horizontal and vertical spatial resolution in the continental lithosphere. In total, the present data set is composed of ~850000 60 s global/NA and ~200000 40 s NA first orbit Rayleigh and Love wave fundamental and overtone wave packets. The waveforms are individually weighted by their amplitude, noise and path redundancy as described in Li and Romanowicz (1996), with the latter factor critically important in properly accounting for irregular sampling across the NA continent introduced by the dense TA site distribution.

The horizontal extent of our model space is defined so as to contain the entire source station paths for all the regional distance data (Fig. 1(b)), which is necessary for modeling the corresponding waveforms using a regional spectral element code, as described below. We parameterize our model space using spherical splines (Wang and Dahlen, 1995), with varying nodal spacing according to the ray path coverage: the 1° nodes roughly correspond to the region covered by the TA sites and the nearest neighboring region, then 2° nodes fill up the rest of continent and margins up to the borders of the model space (Fig. S1). The node spacing is 4° in the region outside of the model space where the model parameters are fixed as in SEMum2 (French et al., 2013), which is used to correct for 3D path effects outside of the model region for the 60 s global and 60 s NA waveforms, and below 1000 km depth for the 40 s NA waveforms. The vertical parameterization comprises 26 B-splines, with a node spacing that varies from 20 km beneath the Moho to 150 km at 1000 km depth (Mégnin and Romanowicz, 2000).

We simultaneously invert for isotropic shear velocity V_s and radial anisotropy ξ along the 3D node grid, by solving an inverse problem with ~70k unknowns using an efficient parallelized scheme (French et al., 2010). The inversion is solved iteratively in the following steps: first, we perform two iterations of NACT inversion (Li and Romanowicz, 1995) starting from SEMum2, and using the global 60 s and 60 s NA datasets to construct the starting model for the new inversion. In this step, both forward and inverse problems are carried out using NACT.

In the second step, we use the spectral element method to accurately compute the forward seismic wavefield in the starting model obtained in step 1, for the 40 s NA data for which the entire path is contained within the model region (Fig. 1(b)). Similarly to the procedure adopted in our recent global tomography studies (Lekić and Romanowicz, 2011; French et al., 2013), to invert for the update of both isotropic V_s and radial anisotropy ξ structure, we use computationally efficient 2D finite frequency kernels based on NACT (Li and Romanowicz, 1996). For paths at distances less than 15°, NACT breaks down and we instead use the classical path average approximation (PAVA) employed in many surface waveform tomographic studies (Woodhouse and Dziewon-ski, 1984). This SEM-based hybrid approach reduces the computational expense of each inversion iteration at least three-fold over adjoint techniques, and also allows for an inversion based on a fast-converging Newton method, requiring fewer iterations overall. We argue (e.g., Lekić and Romanowicz, 2011) that accurate computation of the forward wavefield, and thus also the misfit function, is more important than that of the sensitivity kernels, for which error is of second order, and which can therefore be computed approximately, as long as the starting 3D model already contains the salient long wavelength features of the model.

In this second step of the inversion, we largely mirror the processing performed in the global SEM-based hybrid modeling approach (Lekić and Romanowicz, 2011; French et al., 2013), except the global SEM synthetic code is replaced by a regional Spectral Element code in spherical geometry, RegSEM (Cupillard et al., 2012). RegSEM includes ellipticity, attenuation, and arbitrary anisotropy structure. Most importantly, RegSEM includes PML (Per-

fectly Matched Layer) absorbing boundary conditions, which allow us to restrict the computation laterally and radially to the region of interest.

Because SEM simulations are so precise, we require a model of crustal structure that accurately predicts the seismic response of the earth's crust – particularly for highly sensitive fundamental-mode surface waves. Indeed, fidelity to crustal effects is especially critical for accurate retrieval of anisotropic mantle structure, as often noted when discussing the shortcomings of standard linear crustal corrections (Bozdog and Trampert, 2008; Lekić et al., 2010; Ferreira et al., 2010). Here, we adopt the smooth crustal modeling technique proposed in Lekić and Romanowicz (2011) and later refined by French et al. (2013). The thin layers of the earth's crust slow down SEM computations considerably, particularly in the oceans. To mitigate this effect, we construct models of the crust that contain no interior discontinuities and are potentially thicker than the real crust in some regions. These smooth models are calibrated to mimic the seismic response of the earth's crust, as seen through observations of surface-wave group-velocity dispersion, by introducing crustal radial anisotropy (Backus, 1962; Capdeville and Marigo, 2007).

In the continents, our smooth crust matches the Moho depth of Crust2.0 (Bassin et al., 2000), with slight smoothing to avoid aliasing in the SEM mesh, while Moho depth saturates at 30 km in oceanic regions. A similar technique, but calibrated to mimic the dispersion of an *a priori* crustal model and not restricted to match continental Moho topography, has previously been shown to be effective for regional-scale waveform inversions (Fichtner et al., 2009). The disadvantages of such a technique are: (a) that the crustal model is only valid over the period range it is calibrated, in this case periods at or above 25 s, and (b) susceptibility to noise in the dispersion data upon which it is calibrated. The first concern should not be an issue for the 40 s and 60 s SEM modeling employed here, confirmed in the global and North-American region validation simulations reported by French et al. (2013). To address the second concern, these authors produced ensembles of crustal models calibrated on dispersion data with realistic-amplitude synthetic noise added, and examined variation in the resulting SEM synthetics, concluding that such errors could not significantly affect long-period waveforms. Thus, we are confident that the crustal modeling approach is able to attain SEM speedup, while maintaining fidelity to the observed surface-wave dispersion characterizing crustal structure, and without negatively affecting the resulting long-period fundamental and higher mode waveforms and the resulting upper mantle shear velocity and radial anisotropy structure.

3. Resolution tests

As explained in previous papers (Marone et al., 2007; Yuan et al., 2011), our waveform dataset has significant depth sensitivity to isotropic shear velocity down to the transition zone, owing to the use of higher mode waveforms, while the sensitivity to radial anisotropy drops rapidly below 300 km depth. The RegSEM based step in our process includes shorter period (40 s) data, which provide better depth and lateral resolution especially in the continental lithosphere than previous studies. The dense TA station spacing also greatly improves lateral resolution by providing continuous coverage at 70-km spacing across the continental US (Fig. S2). Given the period range and our data coverage, we expect a lateral resolution of our V_s and ξ models on the order of 200–400 km and 300–600 km, respectively, and apply different horizontal correlation lengths for V_s and for ξ accordingly in our inversion.

We illustrate the resolving power of the inversion by using classical linear resolution analysis (e.g., Tarantola, 2005) with two sets of synthetic models. The first synthetic model is a synthetic

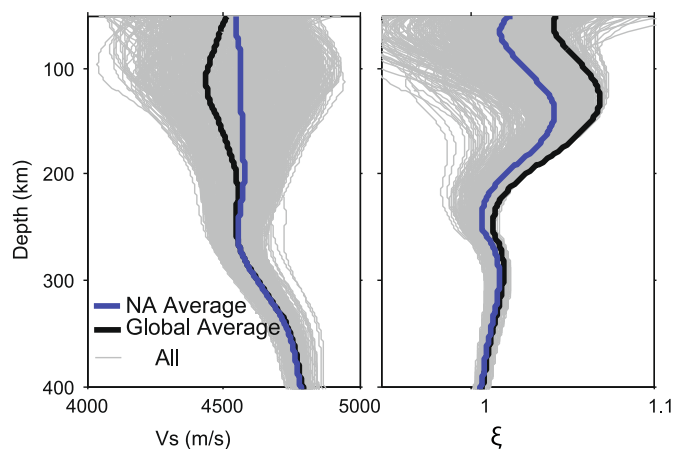


Fig. 2. 1D average depth profiles for isotropic shear velocity (left) and radial anisotropy (right), for the SEMum2 global model (thick black), the regional inversion (thick blue); and depth profiles at all locations in the model (thin gray, background), showing the spread in velocities. The regional averages are distinct from the global averages down to ~ 250 km (see text, Section 4.1). Isotropic velocity and radial anisotropy variations in Figs. 3–6 are with respect to the regional mean (thick blue). (For interpretation of the references to color in this figure legend, the reader is referred to the web version of this article.)

model that exhibits the wide spectrum of seismic structure expected in the continent by taking the starting model in step 2 in Section 2 but swapping the V_s and ξ parameters. In terms of structural pattern, recovery of large scale structure at both lithosphere and asthenosphere depths is excellent (Figs. S3 and S4), while radial anisotropy ξ suffers some degree of amplitude loss at the greater depths. Another synthetic model is composed of spatial “spikes” throughout the model space (e.g., Spakman, 1991; Dueker and Yuan, 2004), which is ideal to investigate spatial blurring or smearing of the model. Fig. S5 shows that specifically in eastern North America the spatial pattern is well recovered without any signs of ray-like horizontal smearing for both V_s and ξ parameters, while the amplitude recovery for ξ , especially at the larger depths, is weaker.

4. Tomographic inversion results and interpretation

The tomographic inversion results for V_s and ξ are presented in Figs. 2–6. We divide the model description and interpretation into two parts, focusing first on the continent-wide structure and then, in more detail, on eastern North America.

4.1. Continental scale model

As noted in our previous continental scale studies (Marone et al., 2007; Yuan et al., 2011), the North American average profiles with depth of V_s and ξ (Fig. 2) are clearly distinct from those of the global model, which is biased towards oceanic structure at shallow depths. On average, the V_s structure is faster than the global average down to 200 km, but shows quite a wide distribution due to inclusion in the model of the thick craton, the Pacific and Atlantic margins, as well as the Western US. The ξ average is larger than 1, but smaller than for the global profile, which again reflects the strong $\xi > 1$ signature of the oceans, which dominates in the global model. The peak of the strong $\xi > 1$ region is slightly deeper than that of the global average. Below 300 km depth, both global and regional average models converge.

4.1.1. Upper mantle structure beneath the craton

At the continental scale, the isotropic V_s images (map views in Fig. 3 and cross sections in Fig. 4) confirm the presence of a thick cratonic root that is characterized by faster than average

V_s down to ~ 200 –250 km, a depth range that in general agrees with the cratonic lithosphere thickness inferred from other studies (e.g., Gung et al., 2003; Griffin et al., 2004; Eaton et al., 2009; O’Reilly and Griffin, 2010; Yuan and Romanowicz, 2010a). Notably, depth cross sections show the low velocity zone is clearly present between ~ 200 and 300 km depth everywhere under the Archean craton (Fig. 4(a), (b)), an observation that may not be common to all cratons (e.g., Pedersen et al., 2009). In addition, the new model exhibits some previously unresolvable details in the cratonic lithosphere, compared to our previous, lower resolution models (Fig. S6). The western edge of the craton is sharply defined across the Rocky Mountain front (which spatially correlates with the Laramide/Cordillera deformation front), best seen above 150 km depth. At 200 km the craton root seems to retract to the center of the continent beneath the Superior craton (see also Fig. 4(b)), and most of the high velocity features seems to vanish beyond 250 km. The outboard of the high velocity craton root thins out to ~ 150 km depth in all Proterozoic provinces (Granite–Rhyolite, Grenville provinces in Fig. 4(a), (b)), and the southwestern leading edge is now under central US. It is interesting to note that the geological limits of the craton crust extend much further west along the western continental rift margin in the western US: for example, Archean to late Proterozoic rocks are sampled in the Mojave crustal province (MJ in Fig. 3; Lee et al., 2001). Widespread slower than average velocities observed in this region suggest that the cratonic root is largely eroded at its western boundary, and a great portion of its Archean lithosphere may have been removed (e.g., Lee et al., 2000).

In eastern North America, east of the Archean/Proterozoic boundary marked by the Grenville front (blue line in Fig. 3; GF in Fig. 4), the high velocity lithosphere is divided into several blocks separated by lower velocities beneath the eastern continental margin (ERM), and the coast line. The map at 100 km depth shows the high velocity craton margin is in best correspondence with the ERM, the surface geological limits of the cratonic crust, on the north, east and southeast edges of the craton (Fig. 3). In particular, a band of low velocities along the eastern edge of the craton separates the high velocity craton root from domains of faster than average velocities which extend into the Atlantic Ocean. Further discussion of this portion of lithosphere structure follows in Section 4.2. The southern edge of the high velocity anomaly is visible at 100 km in central Texas, and retracts to the north at greater depths (see also in Fig. 4b). A finger of faster than average velocities persists east of the continental margin, into the Blake Plateau and the Blake Ridge (Dillon and Popenoe, 1988) north of Florida.

The northeastern craton boundary, on the other hand, follows the fossil rift system in the Labrador sea that separates Greenland from the North American craton (e.g., Chalmers and Pulvertaft, 2001), down to 250 km depth. High velocities of the Greenland lithosphere seem to vanish between 150 and 200 km (see also Fig. 4(b)). However, this region is at the very northern edge of our model space, and may not be as well resolved.

4.1.2. The Trans-Hudson Orogen

At 70 km depth (Fig. 3), we observe slower velocities along the southern portion of the North American craton, including in the states of Montana (MT), Wyoming (WY), Colorado (CO) and below the Trans-Hudson Orogen (THO). Further north, a narrow band of slow velocities follows the THO and turns eastwards with the orogen, north of the Superior craton. The lower velocities are also present near the eastern end of the THO and into New Quebec orogen (NQ; Wardle et al., 1990) in eastern Canada. Along the depth cross-sections in Fig. 4(a), (b), a negative radial anisotropy ξ anomaly, (i.e., V_{sv} faster than V_{sh}) is present beneath the THO. As the largest Proterozoic orogenic belt in the world, the THO played a critical role in compacting the Canadian Shield and the

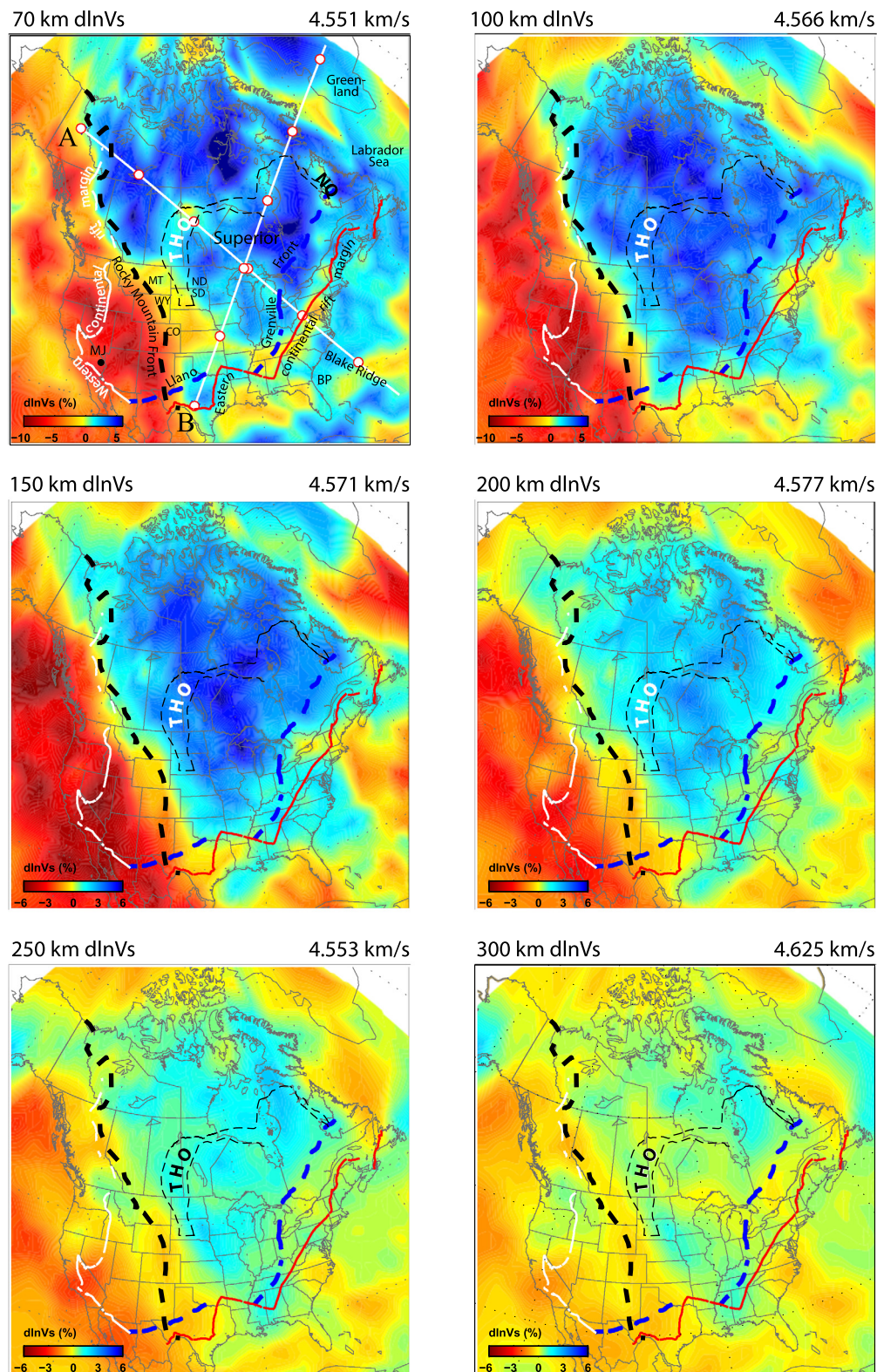


Fig. 3. 3D isotropic shear wave velocity structure of the continent. Map views are shown from 70 km down to 300 km, shown as variations with respect to the regional mean (thick blue line in Fig. 2). Locations of two depth cross-sections shown in Fig. 4 are indicated in (a). Red dots indicate 10° distance mark on the x-axis along each transect (see Fig. 4). Labels are: BP, Blake Plateau; NQ, New Quebec Orogen; THO, Trans-Hudson Orogen. State abbreviations are: CO, Colorado; MT, Montana; ND, North Dakota; SD, South Dakota; and WY, Wyoming. The geological limits of the cratonic crust are indicated as follows: the western continental rift margin (white line) and the eastern continental rift margin (red line); the western edge of the high velocity craton mantle root is marked by the Rocky Mountain front. (For interpretation of the references to color in this figure legend, the reader is referred to the web version of this article.)

North American craton. The North American azimuthal anisotropy study of Yuan and Romanowicz (2010a) shows, at shallow depths (<100 km), systematic alignment of azimuthal anisotropy fast axis

directions with the overall structure trend of the Archean portion of the THO (Fig. 5), and greater thickness (~150 km) of the top layer ("layer 1") of distinct lithospheric azimuthal anisotropy

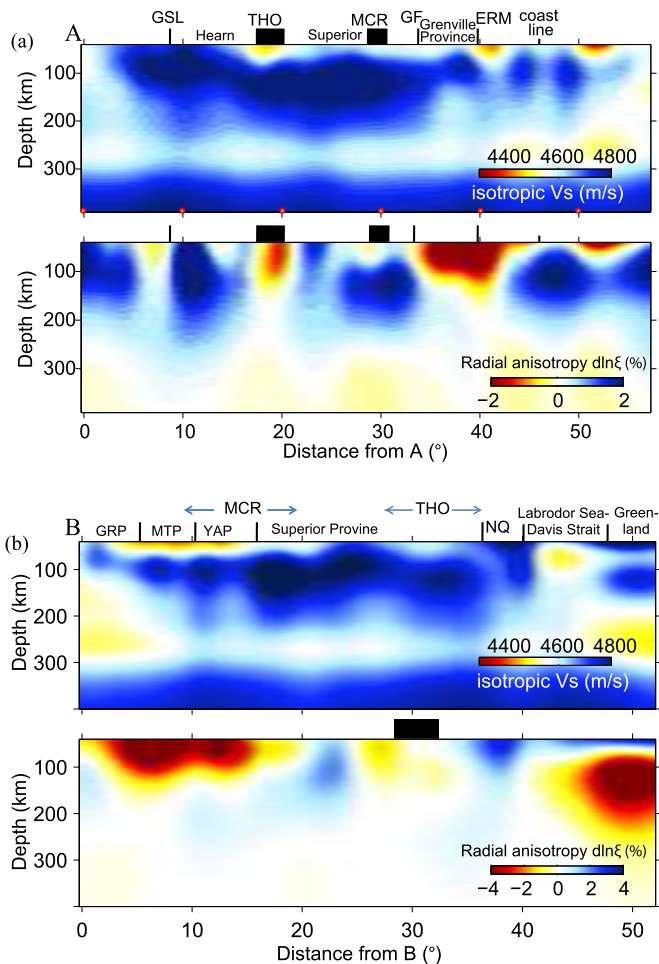


Fig. 4. Depth cross-sections of isotropic V_s (top subpanels) and radial anisotropy variation (bottom subpanels). (a) Profile A: starting from NW Canada. x -axis shows the distance in degrees. Features marked along the cross-sections are: GSL, Great Slave Lake suture zone; THO, Trans-Hudson Orogen; MCR, Mid-Continent Rift; GF, Grenville deformation Front; ERM, eastern continental rift margin. Coastline is indicated. Note the correlation of negative ξ anomaly under all sutures. (b) Profile B from southwest corner of the craton extending into Greenland. GRP, Granite-Rhyolite Province; MTP, Mazatzal Province; YAP, Yavapai Province; MCR, Mid-Continent Rift; THO, Trans-Hudson Orogen; and NQ, New Quebec Orogen.

beneath the THO than in other parts of the craton. It is suggested the transpressional deformation was probably dominant during the time of orogeny in the suture zone lithospheric mantle that separates the THO and adjacent craton blocks (Superior, Hearne and Wyoming). The transpressional deformation caused lattice preferred orientation in the abundant olivine and other anisotropic minerals in the lithospheric mantle to align in a direction parallel to suture-trend, as is generally observed in more recent orogenic belts. These tomographic images, together with similar observations in our earlier generation of the North American model (Yuan et al., 2011) suggest that transpressional deformation during collision processes left relict structural units that are manifested by slower isotropic shear velocity than the surrounding craton lithosphere, and faster V_{sv} than V_{sh} (e.g. negative ξ anomalies) at shallow depths (<100 km).

Deeply extending negative ξ anomalies are also observed under nearly all the main sutures and reworked Proterozoic provinces, e.g., Great Slave Lake suture zone, Grenville deformation front, East Rift Margin, the Grenville province in Fig. 4(a), and Granite/Rhyolite and Yavapai provinces in Fig. 4(b). Fossil subductions along suture zones in the Canadian Shield are inferred from the LithoProbe upper mantle dipping reflectors (van der Velden and Cook, 2005).

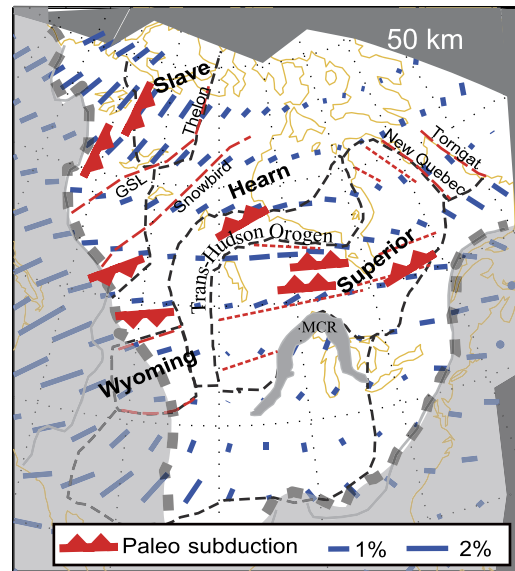


Fig. 5. Paleo-subduction zones, suture trends and shallow depth azimuthal anisotropy fast axis directions plotted on top of the North American Precambrian crustal provinces, modified from Yuan and Romanowicz (2010a). Paleo-subduction directions are inferred from upper mantle dipping reflectors in LithoProbe active source imaging results (van der Velden and Cook, 2005). Thin black dashed lines mark the major crustal provinces. Thick red dashed lines show the major suture zone locations from Hoffman (1988). GSF, Great Slave Lake shear zone. Thinner red dashed lines are sub-provincial terrane boundaries in the Superior craton (Percival et al., 2006). MCR, Mid-Continent Rift. Blue sticks indicate anisotropy fast axis directions at 50 km (Yuan and Romanowicz, 2010a). Note that, within the craton limit (marked by the thick dashed line) the LithoProbe inferred paleo-subduction directions (marked as red symbols) are nearly everywhere parallel to the inverted seismic anisotropy directions. (For interpretation of the references to color in this figure legend, the reader is referred to the web version of this article.)

Beneath all these suture zones, fast axis directions tend to be parallel to the strike of the sutures in the continental-scale azimuthal anisotropy model (Fig. 5), suggesting transpressional deformation may have been preserved widely in the fossil suture zones of the lithosphere. The negative $d\ln\xi$ anomalies observed beneath major sutures also suggest that the suturing processes produced significant vertical sense of shear (i.e., $V_{sv} > V_{sh}$ or negative ξ anomaly) in the lithosphere.

4.2. Central and eastern US

Higher resolution images of the central and eastern US are now available from the new inversion owing to continuous TA coverage reaching the east coast. In addition, the use of 40 s waveforms greatly improves path coverage in this part of the US, as well as in the western portion of the North Atlantic Ocean. Shorter period (40 s) waveforms also provide better depth sensitivity in the craton lithosphere depth range. Figs. 6 and 7 present a detailed view of both the isotropic V_s and ξ model with roughly 2° and 4° lateral resolution, as imposed by the correlation lengths applied.

4.2.1. Mid-continent rift

The 1.1 Ga mid-continent rift system (arcuated black regions in Fig. 6) is an over 2000 km long failed rift system in the central US, formed due to intra-continental extension in response to contraction caused by the Grenville orogeny along the east coast, during the assembly of the Rodinia supercontinent (e.g., Van Schmus and Hinze, 1985; Whitmeyer and Karlstrom, 2007). At 60 km depth (Fig. 6(a)), a correlation is observed between slower than surrounding velocities and nearly all segments/arms of the arcuate rift. This spatial correlation however disappears at greater depths, suggesting that the rift system is represented by a shallow

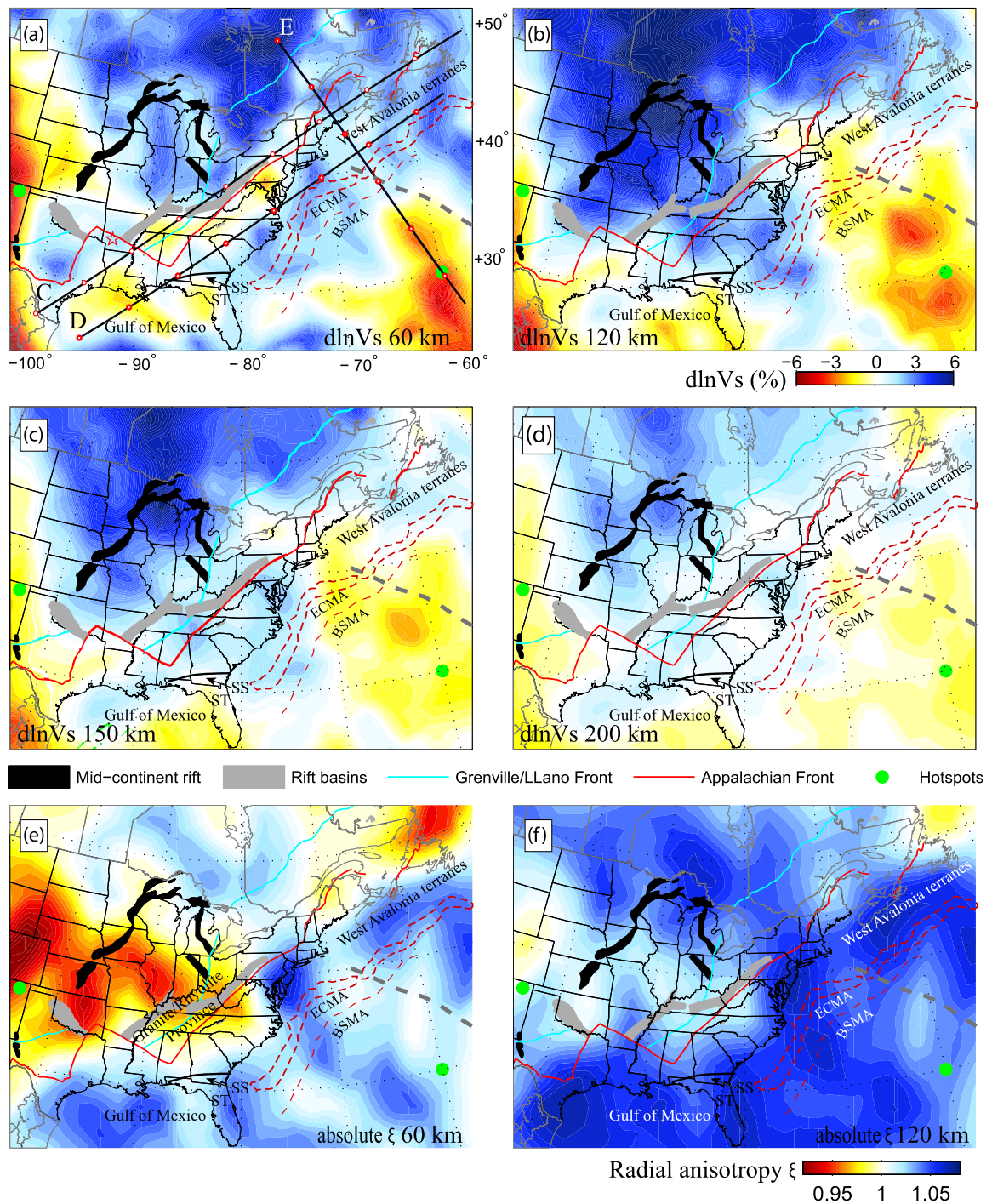


Fig. 6. Lateral variation in isotropic V_s and radial anisotropy structure in eastern North America, shown as variations with respect to the regional mean (thick blue line in Fig. 2). The depth of each map is indicated. Marked surface features are as in Fig. 1, except the Grenville/Llano deformation front is coded in light blue. Green dots are hotspot locations; the Bermuda hotspot is near the lower right corner. Locations of three depth cross-sections in Fig. 7 are also indicated. Top four subpanels are for isotropic V_s ; bottom two are for radial anisotropy ξ . Note the eastern edge of the high velocity craton closely follows the eastern continental margin (red line) at 60 km to 150 km. Labels are: BSMA, Blake Spur Magnetic Anomaly; ECMA, East Coast Magnetic Anomaly; SS, Suwannee Suture; and ST, Suwannee Terrane. (For interpretation of the references to color in this figure legend, the reader is referred to the web version of this article.)

lithospheric feature, at least at the present time. Following the rift, radial anisotropy ξ (>1) is weaker than in the Archean Superior province to the north at 60 km (Fig. 6(e)), but shifting to strong $\xi < 1$ in the Proterozoic terranes to the south (e.g. Granite/Rhyolite province in Fig. 6(e)). In our previous study (Yuan and Romanowicz, 2010a), the mid-continent rift system was also marked by a shallower than average thickness of the top layer ("Layer 1") of lithospheric azimuthal anisotropy.

The continental scale depth cross-sections (Fig. 4) also confirm that beneath the rift slower than average velocities are confined to shallow (<100 km) depth (Fig. 4(a), (b)); higher velocity and positive radial anisotropy ($\xi > 1$) are present at larger depths to the north of the rift (Fig. 4(a), (b)); and prominent $\xi < 1$ anomalies are present deeper than 100 km in the THO (Fig. 4(a), (b)) and the Proterozoic terranes (Granite/Rhyolite province, Figs. 4(b) and 6(a); and Grenville province, Fig. 4(a)).

4.2.2. Grenville province

The 1.3–0.9 Ga Grenville orogen finalized the assembly of the supercontinent Rodinia. The Grenville deformation front (GF) marks the leading edge of the Grenville province towards the craton (light blue line in Fig. 6), while the eastern continental rift margin (red line in Fig. 6) bounds the province to the south. The northern half of the province is characterized by weak positive velocity anomalies at 60 km, but much faster velocity anomalies at 120 and 150 km, similar to what is observed in the Archean lithosphere immediately to the north (Fig. 6(b), (c)); also cross-section E in Fig. 7(c)). This may be an indication of “wedge” tectonics, as proposed along Archean margins from deep seismic reflection studies (e.g., Snyder, 2002): during orogenic events the rheologically stronger Archean lithosphere extrudes into the relatively weaker juvenile (e.g., Proterozoic Grenville) terranes, resulting in a wedge of high velocity Archean lithosphere embedded into the more juvenile block. The Archean lithosphere therefore extends laterally further under the Proterozoic crust.

A large $\xi < 1$ anomaly is observed in the same depth range in this portion of the province (Fig. 4(a); Fig. 7(c)). If the wedge tectonics hypothesis holds and this underlying lithosphere is Archean in origin, it is possible that the Archean lithosphere may have been repeatedly reworked to leave a significant sense of vertical shear in the lithosphere, while on the other hand it still remains fast in velocity, due possibly to its different chemical composition. Alternatively, it was suggested that multiple accretional events occurred during the Rodinia assembly, given the long age span of the orogen (Thomas, 2006). Individual Proterozoic terranes may have been consolidated into part of the craton, but the deformation associated with each accretion episode may well be preserved in the radial anisotropy negative anomaly.

4.2.3. Eastern continental rift margin

As mentioned earlier, the southeast border of the craton is marked by a prominent band of slow velocities at shallow depth (Fig. 6(a)) that roughly follows the eastern continental rift margin (red line in Fig. 6), which also correlates spatially with the New York–Alabama magnetic lineament (not shown; see King and Zietz, 1978). The rift margin was developed during the breakup of Rodinia to form the Iapetus Ocean, and at the present time marks the easternmost extent of North American (Laurentia) continental rocks: to the east of the margin are terranes accreted to the stable Laurentia core in Permian time, during the Appalachian orogen which closed the Iapetus Ocean and assembled the supercontinent Pangea. The terranes were later left behind when Pangea broke apart and the Atlantic Ocean opened (Thomas, 2006; Whitmeyer and Karlstrom, 2007; Bartholomew and Hatcher, 2010). This series of Appalachian orogenic processes seems to have left a slow velocity signature that is of lithospheric scale, given the deep reach of the slow anomaly present in the current (at least 150 km in Fig. 6(c); see also depth cross-section C in Fig. 7(a)) and also in early tomographic studies (e.g., Romanowicz, 1979; van der Lee and Nolet, 1997).

4.2.4. Exotic terranes

The fast velocity structure east of the continental rift margin corresponds to the Proterozoic Gondwanian terranes of pan-African affinity, e.g. from the Suwannee terrane in Florida (Smith, 1982) up to the west Avalonia terranes (Fig. 6) in the Canadian Appalachians in the northeast (e.g., Nance et al., 2002). High velocities of the accreted terranes are in good agreement with their proposed Proterozoic continental origin. This persistent pattern of accreted terranes that remained attached to the North American margin during the opening of the Atlantic is clearly traced in Atlantic fracture zones at the surface (see Thomas, 2006). The observation of fast velocities northwest of the Suwannee structure (SS in Fig. 6(c))

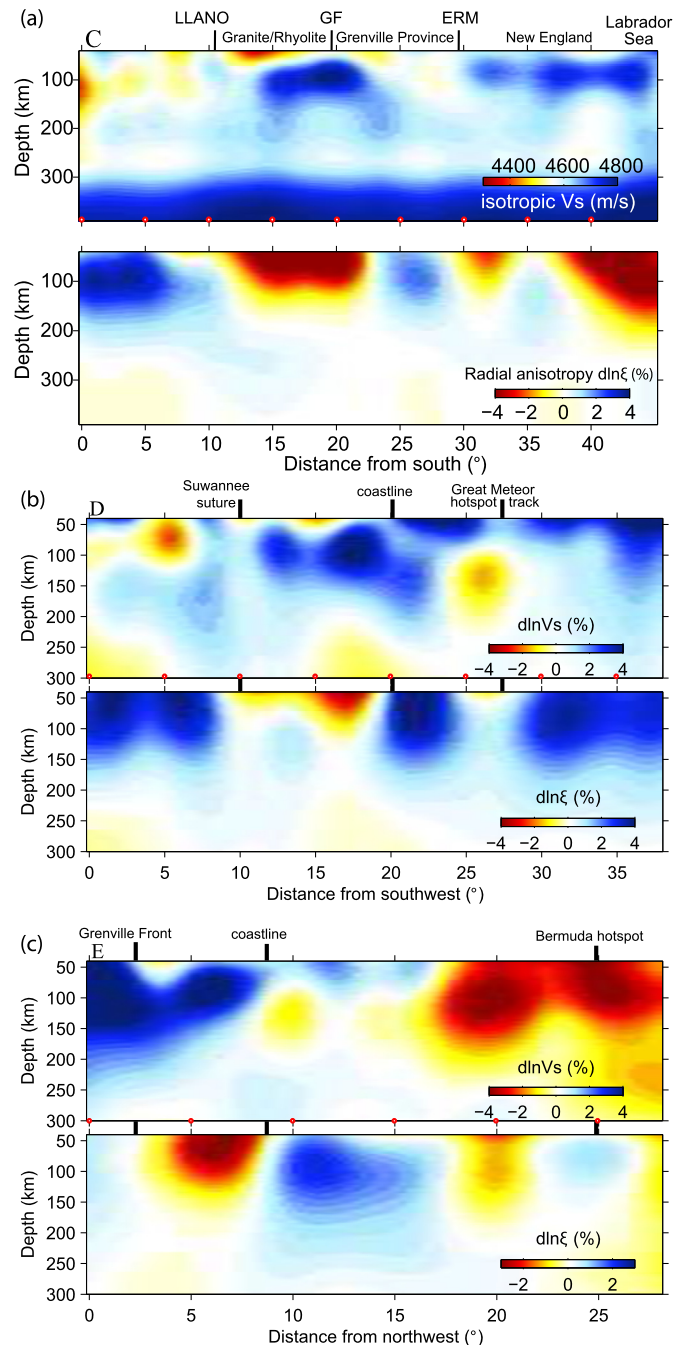


Fig. 7. Depth cross-sections along the lines shown in Fig. 6(a), showing absolute isotropic velocity variations (top subpanels) and radial anisotropy variations (bottom subpanels). (a) Profile C sampling the low velocity band following the ERM. GF, Grenville Front; ERM, Eastern continental rift margin. (b) Profile D from Gulf of Mexico to Newfoundland in east Canada sampling the accreted terranes outboard of the east continent rift. Key structural features along the surface are indicated. (c) Profile E from east Superior to the Bermuda hotspot. Note the deep origin of the low velocity channel beneath the hotspot.

and beyond the coastline, continuing up north to the west Avalonian terranes, persisting down as deep as 150 km (Fig. 6(c); and depth cross-section D in Fig. 7(b)), suggests these exotic terranes extend deep into the lithosphere.

The Atlantic limit of the high velocities reaches the East Coast Magnetic Anomaly (ECMA) and the Blake Spur Magnetic Anomaly (BSMA in Fig. 6(c); e.g., Labails et al., 2010). The ECMA is a strong positive magnetic anomaly, which follows the spatial offset of the

Laurentia rifted margin continuously (except that it is truncated near the Great Meteor hotspot track, indicated Fig. 6; see discussion about the hotspot track below), and is thought to represent the continent–ocean passive margin, as typical oceanic crust is observed beyond this limit (Holbrook et al., 1994). The BSMA is a less prominent positive magnetic anomaly, which is 150- to 250-km seaward of the ECMA and is thought to represent either a ridge jump (Vogt, 1973) or a rapid change in plate motion direction and in spreading rate at the time of the Atlantic ocean opening up (Labails et al., 2010). Spatial continuation of the high velocities to at least east of the ECMA suggests that these accreted terranes are also large in volume.

Observations of large volume terranes of continent-affinity are not uncommon. On the African side of the Atlantic, in situ Re–Os analysis of sulfide grains in mantle-derived xenoliths in the Cape Verde Islands, 500-km offshore western Africa, shows that the xenoliths represent a portion of continental lithospheric mantle that is dated Neoproterozoic to Archean (Coltorti et al., 2010). These data, along with the high velocity tomographic feature present in the upper 100 km of the region (Begg et al., 2009), suggest that a fragment of ancient continental lithosphere, probably African in origin, may be embedded in the Atlantic oceanic lithosphere (Coltorti et al., 2010). South of the Laurentia margin in North America, Archean sub-continental lithosphere is also sampled beneath Prairie Creek in Arkansas (red star in Fig. 5(a)), with inferred age from Re–Os analysis up to 3.4 Ga (Griffin et al., 2011), suggesting a piece of the remnant Archean continent was accreted to the southern edge of the North American craton.

4.2.5. Bermuda low velocity channel

The brightest feature in Fig. 6 is the low velocity anomaly in the northwest Atlantic (southeast corner of the maps), which continues to at least 200 km depth. The anomaly is broad at depth but gradually narrows to the surface. The surface projection of the low velocity anomaly overlaps with the location of the Bermuda hotspot, and we therefore refer to this feature as “the Bermuda low velocity channel”. The northeast edge of the low velocity channel also seems to correlate with the Great Meteor/New England seamount chain in the Atlantic (marked as a broken line in Fig. 6(c)), and may indicate a connection between the deep low velocities and the seamounts on the surface. It is proposed the Great Meteor sea mount chain is further projected inland into the North American continent (e.g., Eaton and Frederiksen, 2007). An indentation, or a ‘divot’, near the base of the cratonic lithosphere was observed in earlier tomographic studies (e.g., van der Lee and Nolet, 1997), and was interpreted as a result of the passage of North America over a hotspot associated with the Great Meteor seamounts (Rondenay et al., 2000). Our isotropic velocity images confirm the presence of the low velocities both inland and offshore, but also show that, in the Atlantic, the trend of the low velocity channel departs from that of the Great Meteor/New England seamount chain. The low velocity channel extends below 250 km near the Bermuda hotspot, and seems to connect with one of the global low velocity fingers seen in the global SEM-based tomography in this depth range (French et al., 2013), which extends further east in the Atlantic.

In the radial anisotropy maps (Fig. 6(e), (f)), the northwest trending low velocity channel is expressed by a relatively weak $V_{sh} > V_{sv}$ pattern. Compared with the large surrounding region of $\xi > 1$ in the Northwest Atlantic, this weak $\xi > 1$ anomaly may reflect the northwest migration of the low velocity channel that weakened and eroded its way up into the oceanic lithosphere and produced a significant vertical component of shear in the shallow lithosphere (visible as deep as 120 km in Fig. 6(f)).

5. Concluding remarks

Our new higher resolution model of the North American upper mantle, based on 40 s regional waveforms and wavefield computations using the spectral element method presents several notable features. In the central part of the craton, rather uniform thickness of the high velocity lithosphere (200–250 km) is observed, confirming earlier results based on azimuthal anisotropy tomography (Yuan and Romanowicz, 2010a). The high velocity root is thickest beneath the core part of the craton, the Superior province, and thins towards its margins. Under the Proterozoic regions of the craton in the US, the thickness of the root decreases to between 150 and 100 km. In the upper mantle, the craton is bounded by the eastern continental rift margin in the east, consistent with the surface limits of the cratonic crust. In contrast, the western edge of the craton root closely follows the Rocky Mountains, while on the surface, the craton crust reaches out further to the western continental rift margin, suggesting a large chunk of the Precambrian lithosphere in the western US is currently removed. Similarly to what is observed in the Yuan et al. (2011) model, radial anisotropy in the Proterozoic suture zones is always weaker than in the surrounding Archean lithosphere, suggesting vertical sense of shear related to the deformation is well preserved in the suture zone lithosphere. Compared with the Archean lithosphere, the younger Proterozoic Granite/Rhyolite and Grenville provinces are also characterized by strong negative $d \ln \xi$, representing repeatedly reworked cratonic lithosphere.

In eastern North America, the lateral variations of shear velocity and radial anisotropy do not present the spatial continuity seen in the Archean lithosphere further to the west (e.g. Fig. 4). Instead, they express the preservation, not only in the surface geology and crustal structure, but also in the deeper lithosphere, of major orogenic events as well as many intra-orogenic extensional events (e.g., the Mid-Continent Rift system) and thrust events, reflecting the rich tectonic history of this part of the continent, namely two episodes of full Wilson cycles that are evident along the continental margin (e.g., Thomas, 2006), as recorded by the Grenville and Appalachian orogens. The Grenville orogeny marked the formation of the supercontinent Rodinia by closing a pre-Rodinia ocean. Breakup of Rodinia opened up the Iapetus Ocean, which was closed later following the succeeding Appalachian orogeny that formed the supercontinent Pangea. Breakup of Pangea consequently opened up the current Atlantic Ocean.

The cratonic root has been affected by recurring episodes of tectonism, however its eastern margin seems largely intact west of the Grenville deformation front. The Archean lithosphere may have extended further outboard of the Proterozoic Grenville deformation front, as indicated by high velocity Archean-like structure that extruded beyond the deformation front. Across the continental margin, slower than average velocities are observed at ~100 km depth, indicating a thinned lithosphere sandwiched between the Archean core and the thick exotic terranes further offshore that are of suggested continental origin. In the northeastern US thinner lithosphere along the low velocity band is reported in discontinuity sensitive receiver functions (Rychert et al., 2007; Yuan and Levin, submitted for publication). Several local velocity studies (e.g., Rayleigh wave dispersion inversion, Li et al., 2003; non-plane surface-wave imaging, Pollitz and Mooney, 2013; and P-waveform modeling, Chu et al., 2013) report the presence of low velocities in sporadic locations from northeastern US to the New Madrid seismic zone, which spatially agree with our observations. The low velocity zone along the continental margin intersects the New England and the Bermuda low velocity channel, a prominent low velocity feature which initiated deep near the Bermuda hotspot in the Atlantic Ocean, although it seems to extend further east into younger Atlantic Ocean (French et al., 2013). The Bermuda

low velocity channel has clearly cut its way into the craton where it has reached the Grenville deformation front. In contrast to this fragmented incursion, the southwestern margin of the North American craton has been effectively altered. There, the high velocity root is now closely bounded by the Laramide/Cordilleran deformation front (Figs. 3, 4).

The new tomographic image of eastern North America suggests the presence of deeply rooted (>150 km) Gondwanian blocks. While somewhat thinner than the Archean lithosphere in the center of the craton, these blocks may have been captured during the North American/African collision that closed the Iapetus Ocean, but stayed behind when the present Atlantic Ocean was formed (Smith, 1982; Nance and Murphy, 1994; Dennis and Wright, 1997; Hibbard et al., 2002). The exotic terranes are clearly separated from the Laurentia core along the east continent margin, and extend greatly outboard into the Atlantic Ocean, reaching out to the oldest Atlantic oceanic crust (i.e., EAMA and BSMA). The presence of large segments of fossil continents off cratonic margins is thus not uncommon, and may suggest that they played an important role in the global crustal-growth episodes (Griffin et al., 2011).

Acknowledgements

The IRIS data management center is thanked for providing the waveforms used in this study. This project was partially supported by NSF grant EAR-1135452. We acknowledge the support by iVEC, Australia through the use of advanced computing, and the support at the National Energy Research Scientific Computing Center by the U.S. Department of Energy Office of Science, contract DE-AC02-05CH11231. B.R. acknowledges support from the European Research Council under the E.C.'s 7th Framework program (FP7-IDEAS-ERC)/ERC Advanced grant "WAVETOMO". This is a BSL contribution: Number 13-15.

Appendix A. Supplementary material

Supplementary material related to this article can be found online at <http://dx.doi.org/10.1016/j.epsl.2013.11.057>.

References

- Backus, G.E., 1962. Long-wave elastic anisotropy produced by horizontal layering. *J. Geophys. Res.* 67, 4427–4440.
- Bartholomew, M.J., Hatcher Jr., R.D., 2010. The Grenville orogenic cycle of southern Laurentia: Unraveling sutures, rifts, and shear zones as potential piercing points for Amazonia. *J. South Am. Earth Sci.* 29, 4–20.
- Bassin, C., Laske, G., Masters, G., 2000. The current limits of resolution for surface wave tomography in North America. *Eos Trans. AGU* 81, F897.
- Bedle, H., van der Lee, S., 2009. S velocity variations beneath North America. *J. Geophys. Res.* 114.
- Begg, G.C., Griffin, W.L., Natapov, L.M., O'Reilly, S.Y., Grand, S.P., O'Neill, C.J., Hronsky, J.M.A., Djomani, Y.P., Swain, C.J., Deen, T., Bowden, P., 2009. The lithospheric architecture of Africa: Seismic tomography, mantle petrology, and tectonic evolution. *Geosphere* 5, 23–50.
- Bozdag, E., Trampert, J., 2008. On crustal corrections in surface wave tomography. *Geophys. J. Int.* 172, 1066–1082.
- Capdeville, Y., Marigo, J.J., 2007. Second order homogenization of the elastic wave equation for non-periodic layered media. *Geophys. J. Int.* 170, 823–838.
- Chalmers, J.A., Pulvertaft, T.C.R., 2001. Development of the continental margins of the Labrador Sea: a review. In: *Special Publications*, vol. 187. Geological Society, London, pp. 77–105.
- Chu, R., Schmandt, B., Helmberger, D.V., 2012. Upper mantle P velocity structure beneath the Midwestern United States derived from triplicated waveforms. *Geochem. Geophys. Geosyst.* 13, Q0AK04.
- Chu, R., Leng, W., Helmberger, D.V., Gurnis, M., 2013. Hidden hotspot track beneath the eastern United States. *Nat. Geosci.* 6, 963–966. <http://dx.doi.org/10.1038/ngeo1949>.
- Coltorti, M., Bonadiman, C., O'Reilly, S.Y., Griffin, W.L., Pearson, N.J., 2010. Buoyant ancient continental mantle embedded in oceanic lithosphere (Sal Island, Cape Verde Archipelago). *Lithos* 120, 223–233.
- Cupillard, P., Delavaud, E., Burgos, G., Festa, G., Vilotte, J.-P., Capdeville, Y., Montagner, J.-P., 2012. RegSEM: a versatile code based on the spectral element method to compute seismic wave propagation at the regional scale. *Geophys. J. Int.* 188, 1203–1220.
- Darbyshire, F.A., Lebedev, S., 2009. Rayleigh wave phase-velocity heterogeneity and multilayered azimuthal anisotropy of the Superior Craton, Ontario. *Geophys. J. Int.* 176, 215–234.
- Dennis, A.J., Wright, J.E., 1997. The Carolina terrane in northwestern South Carolina, USA: Late Precambrian–Cambrian deformation and metamorphism in a peri-Gondwanan oceanic arc. *Tectonics* 16, 460–473.
- Dillon, W.P., Popenoe, P., 1988. The Blake Plateau Basin and Carolina Trough. In: Sheridan, R.E., Grow, J.A. (Eds.), *The Atlantic Continental Margin, U.S. (The Geology of North America)*. Geological Society of America.
- Dueker, K.G., Yuan, H., 2004. Upper mantle P-wave velocity structure from PASS-CAL teleseismic transects across Idaho, Wyoming and Colorado. *Geophys. Res. Lett.* 34. <http://dx.doi.org/10.1029/2004GL019476>.
- Eaton, D.W., Frederiksen, A., 2007. Seismic evidence for convection-driven motion of the North American plate. *Nature* 446, 428–431.
- Eaton, D.W., Darbyshire, F., Evans, R.L., Grütter, H., Jones, A.G., Yuan, X., 2009. The elusive lithosphere–asthenosphere boundary (LAB) beneath cratons. *Lithos* 109, 1–22.
- Ferreira, A.M.G., Woodhouse, J.H., Visser, K., Trampert, J., 2010. On the robustness of global radially anisotropic surface wave tomography. *J. Geophys. Res., Solid Earth* 115, B04313.
- Fichtner, A., Kennett, B.L.N., Igel, H., Bunge, H.-P., 2009. Full seismic waveform tomography for upper-mantle structure in the Australasian region using adjoint methods. *Geophys. J. Int.* 179, 1703–1725.
- Frederiksen, A.W., Bollmann, T., Darbyshire, F., van der Lee, S., 2013. Modification of continental lithosphere by tectonic processes: A tomographic image of central North America. *J. Geophys. Res., Solid Earth* 118, 1051–1066.
- French, S.W., Lekić, V., Romanowicz, B., 2010. Toward the Future of Global Waveform Tomography: Scalable Gauss–Newton and Alternative Data-Partitioning Schemes. *Berkeley Seismological Laboratory Annual Report* 34–35.
- French, S.W., Lekić, V., Romanowicz, B., 2013. Waveform tomography reveals channeled flow at the base of the oceanic asthenosphere. *Science* 342, 227–230.
- Griffin, W.L., O'Reilly, S.Y., Doyle, B.J., Pearson, N.J., Coopersmith, H., Kivi, K., Malkovets, V., Pokhilenko, N., 2004. Lithosphere mapping beneath the North American plate. *Lithos* 77, 873–922.
- Griffin, W.L., Begg, G.C., Dunn, D., O'Reilly, S.Y., Natapov, L.M., Karlstrom, K., 2011. Archean lithospheric mantle beneath Arkansas: Continental growth by microcontinent accretion. *Geol. Soc. Am. Bull.* 123, 1763–1775.
- Gung, Y., Panning, M., Romanowicz, B., 2003. Global anisotropy and the thickness of continents. *Nature* 422, 707–711.
- Hibbard, J.P., Stoddard, E.F., Secor, D.T., Dennis, A.J., 2002. The Carolina Zone: overview of Neoproterozoic to Early Paleozoic peri-Gondwanan terranes along the eastern flank of the southern Appalachians. *Earth-Sci. Rev.* 57, 299–339.
- Hoffman, P.F., 1988. United plates of America, the birth of a craton: Early proterozoic assembly and growth of Laurentia. *Annu. Rev. Earth Planet. Sci.* 16, 543–603.
- Holbrook, W.S., Purdy, G.M., Sheridan, R.E., Glover, L., Talwani, M., Ewing, J., Hutchinson, D., 1994. Seismic structure of the U.S. Mid-Atlantic continental margin. *J. Geophys. Res., Solid Earth* 99, 17871–17891.
- King, E.R., Zietz, I., 1978. The New York–Alabama lineament: Geophysical evidence for a major crustal break in the basement beneath the Appalachian basin. *Geology* 6, 312–318.
- Labails, C., Olivet, J.-L., Aslanian, D., Roest, W.R., 2010. An alternative early opening scenario for the Central Atlantic Ocean. *Earth Planet. Sci. Lett.* 297, 355–368.
- Lee, C.-T., Yin, Q., Rudnick, R.L., Chesley, J.T., Jacobsen, S.B., 2000. Osmium isotopic evidence for mesozoic removal of lithospheric mantle beneath the Sierra Nevada, California. *Science* 289, 1912–1916.
- Lee, C.-T., Yin, Q., Rudnick, R.L., Jacobsen, S.B., 2001. Preservation of ancient and fertile lithospheric mantle beneath the southwestern United States. *Nature* 411, 69–73.
- Lekić, V., Romanowicz, B., 2011. Inferring upper-mantle structure by full waveform tomography with the spectral element method. *Geophys. J. Int.* 185, 799–831.
- Lekić, V., Panning, M., Romanowicz, B., 2010. A simple method for improving crustal corrections in waveform tomography. *Geophys. J. Int.* 182, 265–278.
- Levin, V., Park, J., Brandon, M.T., Menke, W., 2000. Thinning of the upper mantle during late Paleozoic Appalachian orogenesis. *Geology (Boulder)* 28, 239–242.
- Li, A., Forsyth, D.W., Fischer, K.M., 2003. Shear velocity structure and azimuthal anisotropy beneath eastern North America from Rayleigh wave inversion. *J. Geophys. Res.* 108, 24 pp.
- Li, X., Romanowicz, B., 1996. Global mantle shear velocity model developed using nonlinear asymptotic coupling theory. *J. Geophys. Res.* 101, 22245–22273.
- Li, X.-D., Romanowicz, B., 1995. Comparison of global waveform inversions with and without considering cross-branch modal coupling. *Geophys. J. Int.* 121, 695–709.
- Marone, F., Romanowicz, B., 2007. The depth distribution of azimuthal anisotropy in the continental upper mantle. *Nature* 447, 198–201.
- Marone, F., Gung, Y., Romanowicz, B., 2007. Three-dimensional radial anisotropic structure of the North American upper mantle from inversion of surface waveform data. *Geophys. J. Int.* 171, 206–222.

- Mégnin, C., Romanowicz, B., 2000. The three-dimensional shear velocity structure of the mantle from the inversion of body, surface and higher-mode waveforms. *Geophys. J. Int.* 143, 709–728.
- Menke, W., Levin, V., 2002. Anomalous seaward dip of the lithosphere–asthenosphere boundary beneath northeastern USA detected using differential-array measurements of Rayleigh waves. *Geophys. J. Int.* 149, 413–421.
- Nance, R.D., Murphy, J.B., 1994. Contrasting basement isotopic signatures and the palinspastic restoration of peripheral orogens: Example from the Neoproterozoic Avalonian–Cadomian belt. *Geology* 22, 617–620.
- Nance, R.D., Murphy, J.B., Keppie, J.D., 2002. A Cordilleran model for the evolution of Avalonia. *Tectonophysics* 352, 11–31.
- Nettles, M., Dziewoński, A.M., 2008. Radially anisotropic shear velocity structure of the upper mantle globally and beneath North America. *J. Geophys. Res.* 113.
- O'Reilly, S.Y., Griffin, W.L., 2010. The continental lithosphere–asthenosphere boundary: Can we sample it? *Lithos* 120, 1–13.
- Pedersen, H.A., Fishwick, S., Snyder, D.B., 2009. Comparison of cratonic roots through consistent analysis of seismic surface waves. *Lithos* 109, 81–95.
- Percival, J.A., Sanborn-Barrie, M., Skulski, T., Stott, G.M., Helmstaedt, H., White, D.J., 2006. Tectonic evolution of the western Superior Province from NATMAP and Lithoprobe studies. *Can. J. Earth Sci.* 43 (7). <http://dx.doi.org/10.1139/E1106-1062>.
- Pollitz, F.F., Mooney, W.D., 2013. Seismic structure of the Central US crust and shallow upper mantle: Uniqueness of the Reelfoot Rift. *Earth Planet. Sci. Lett.* <http://dx.doi.org/10.1016/j.epsl.2013.05.042>.
- Romanowicz, B.A., 1979. Seismic structure of the upper mantle beneath the United States by three-dimensional inversion of body wave arrival times. *Geophys. J. R. Astron. Soc.* 57, 479–506.
- Rondenay, S., Bostock Michael, G., Hearn Thomas, M., White Donald, J., Ellis Robert, M., 2000. Lithospheric assembly and modification of the SE Canadian Shield; Abitibi–Grenville teleseismic experiment. *J. Geophys. Res.* 105, 13735–13754.
- Rychert, C.A., Rondenay, S., Fischer, K.M., 2007. P-to-S and S-to-P imaging of a sharp lithosphere–asthenosphere boundary beneath eastern North America. *J. Geophys. Res.* 112, B08314.
- Smith, D.L., 1982. Review of the tectonic history of the Florida basement. *Tectonophysics* 88, 1–22.
- Snyder, D.B., 2002. Lithospheric growth at margins of cratons. *Tectonophysics* 355, 7–22.
- Spakman, W., 1991. Delay-time tomography of the upper mantle below Europe, the Mediterranean and Asia Minor. *Geophys. J. Int.* 107, 309–332.
- Tarantola, A., 2005. *Inverse Problem Theory and Methods for Model Parameter Estimation*. Society for Industrial and Applied Mathematics.
- Thomas, W.A., 2006. Tectonic inheritance at a continental margin. *GSA Today* 16. <http://dx.doi.org/10.1130/1052-5173>.
- van der Lee, S., Nolet, G., 1997. Seismic image of the subducted trailing fragments of the Farallon Plate. *Nature* 386, 266–269.
- van der Velden, A.J., Cook, F.A., 2005. Relict subduction zones in Canada. *J. Geophys. Res.* 110.
- Van Schmus, W.R., Hinze, W.J., 1985. The midcontinent rift system. *Annu. Rev. Earth Planet. Sci.* 13, 345–383.
- Vogt, P.R., 1973. Early events in the opening of the North Atlantic. In: Tarling, D.H., Runcorn, S. (Eds.), *Implications of Continental Drift to the Earth Science*, vol. 2. Academic Press, pp. 693–712.
- Wang, Z., Dahlen, F.A., 1995. Spherical-spline parameterization of three-dimensional Earth models. *Geophys. Res. Lett.* 22, 3099–3102.
- Wardle, R.J., Ryan, B., Ermanovics, I., 1990. The Eastern Churchill Province, Torngat and New Québec orogens: An overview. *Geosci. Canada, [S.I.]* (ISSN 1911-4850) (dec. 1990).
- Whitmeyer, S.J., Karlstrom, K.E., 2007. Tectonic model for the Proterozoic growth of North America. *Geosphere* 3, 220–259.
- Woodhouse, J.H., Dziewoński, A.M., 1984. Mapping the upper mantle: Three-dimensional modeling of earth structure by inversion of seismic waveforms. *J. Geophys. Res., Solid Earth* 89, 5953–5986.
- Yuan, H., Levin, V., submitted for publication. Stratified seismic anisotropy and the lithosphere–asthenosphere boundary beneath Eastern North America. *J. Geophys. Res.*
- Yuan, H., Romanowicz, B., 2010a. Lithospheric layering in the North American craton. *Nature* 466, 1063–1068.
- Yuan, H., Romanowicz, B., 2010b. Depth dependent azimuthal anisotropy in the western US upper mantle. *Earth Planet. Sci. Lett.* 300, 385–394.
- Yuan, H., Romanowicz, B., Fischer, K.M., Abt, D., 2011. 3-D shear wave radially and azimuthally anisotropic velocity model of the North American upper mantle. *Geophys. J. Int.* 184, 1237–1260.